Journal of the Optical Society of America A
OPTICS, IMAGE SCIENCE, AND VISION

Effect of eccentricity and light level on the timing of light adaptation mechanisms

Pablo A. Barrionuevo,[1,*] Beatriz M. Matesanz,[2] Alejandro H. Gloriani,[3] Isabel Arranz,[2] Luis Issolio,[1,4] Santiago Mar,[2] and Juan A. Aparicio[2]

[1]Instituto de Investigación en Luz, Ambiente y Visión, CONICET-UNT, Av. Independencia 1800, San Miguel de Tucumán, T4002BLR Tucumán, Argentina
[2]Departamento de Física Teórica, Atómica y Óptica, Facultad de Ciencias, Universidad de Valladolid, P° Belén 7, 47011 Valladolid, Spain
[3]Fachbereich Psychologie, Philipps-Universität Marburg, Gutenbergstr. 18, 35032 Marburg, Germany
[4]Departamento de Luminotecnia, Luz y Visión, Universidad Nacional de Tucumán, Av. Independencia 1800, San Miguel de Tucumán, T4002BLR Tucumán, Argentina
*Corresponding author: pbarrionuevo@herrera.unt.edu.ar

Received 3 November 2017; revised 4 January 2018; accepted 24 January 2018; posted 26 January 2018 (Doc. ID 312458); published 27 February 2018

We explored the complexity of the light adaptation process, assessing adaptation recovery (*Ar*) at different eccentricities and light levels. Luminance thresholds were obtained with transient background fields at mesopic and photopic light levels for temporal retinal eccentricities (0°–15°) with test/background stimulus size of 0.5°/1° using a staircase procedure in a two-channel Maxwellian view optical system. *Ar* was obtained in comparison with steady data [Vis. Res. 125, 12 (2016)]. Light level proportionally affects *Ar* only at fovea. Photopic extrafoveal thresholds were one log unit higher for transient conditions. Adaptation was equally fast at low light levels for different retinal locations with variations mainly affected by noise. These results evidence different timing in the mechanisms of adaptation involved.

OCIS codes: (330.4060) Vision modeling; (330.7320) Vision adaptation; (330.5310) Vision - photoreceptors.

https://doi.org/10.1364/JOSAA.35.00B144

1. INTRODUCTION

Light adaptation mechanisms allow the visual system to work optimally in a large range of light levels. These mechanisms are contained in the first stage of the visual system, that is, the retina [1–3]. One of the main adaptive mechanisms is related to the photoreceptoral system involved. At high light levels, cones, which allow color and detailed vision, are the only active photoreceptors due to the saturation of rods; this is called photopic vision. On the other hand, scotopic vision is defined when light levels are low enough such that cones become insensitive and only the highly sensitive rods are working. At intermediate light levels, both rods and cones are normally photosensitive and work together, even sharing retinal pathways; this constitutes mesopic vision [4]. The retina is constantly exposed to dynamic input because of head and eye movements and also due to motion elements in the scene; therefore, retinal cells receive a fast gamut of contrasts and light levels. In order to account for this dynamic input, photoreceptors and retinal downstream pathways have fast light adaptation mechanisms [3,5].

Classical psychophysical studies used threshold versus intensity (TvI) curves to identify adaptation mechanisms [6–8]. These studies analyzed adaptation using a just detectable stimulus at different background intensities. Three different mechanisms were proposed by this group of studies. The first one is a multiplicative mechanism, which scales all light in the field by a common factor, in this way modifying the sensitivity to detect a probe according the background level [9,10]. The second proposed mechanism removes steady background signals, and it is called the subtractive mechanism [11–13]. The third mechanism is a nonlinear stage, which compresses the response in order to make it suitable for the neuron's dynamic range. The neuronal circuits that account for these mechanisms were then identified by physiological approaches and incorporated in modern and more complete light adaptation models [9,13–16]. Nevertheless, these approaches did not deal with variations of retinal behavior due to changes in eccentricity.

It is well known that retinal position exerts a large influence on sensitivity at different light levels [17]. One of the main reasons for this behavior is the different distribution of rods and cones across the retina [18,19], but also other findings showed that physiological properties of photoreceptors and bipolar and ganglion cells vary significantly across the retina; e.g., [19–21]. However how light adaptation processing depends on retinal location is not well understood.

On the other hand, with mesopic and photopic vision, TvI curves usually follow Weber's law, which means that the incremental threshold is proportional to the intensity of the background. This behavior is predominant in the luminance channel [22,23]. However, some conditions alter this behavior; for example, for brief and small flashes, luminance thresholds and suprathresholds rise with the square root of the background level, which is known as Rose–de Vries law [24]. Our previous study showed that deviations of Weber's law are not only dependent on test/background relations but also on eccentricity [16]. For a 10° background field, data followed Weber's law with both 0.45° and 2° test fields; considering eccentricities from the fovea to 15° temporal retinal position. However, when the background field size was reduced to 1°, preserving test field size of 0.45°, TvI curves failed to follow Weber's law, particularly at eccentricities higher than 6° [16].

In a similar way in which visual illusions can help in the study of other attributes of the visual system, some stimuli conditions can unveil the visual mechanism processing involved in adaptation, at least partially. For example, comparison of results for different stimuli sizes have helped to relate subtractive mechanism effects with increments of dendritic field sizes of horizontal cells with eccentricity and to explain the involvement of noise in light adaptation for steady conditions [16]. In the current work, we used a classical psychophysical approach to better understand the complexity of the dynamics of light adaptation.

We used the concept of adaptation recovery, which relates threshold with a steadily adapting field and threshold with a transient background, to analyze the effect of eccentricity and light level on the dynamics of light adaptation processing. In this way, we explored light adaptation in three dimensions: space, time, and intensity.

2. METHODS

A. Experimental Setup

A two-channel Maxwellian view optical system was employed, which was previously described elsewhere [25]. Briefly, two concentric beams reached the observer's pupil: a background beam (with luminance L_b) and a probe (with luminance ΔL). Henceforth, we will refer to the spatial region where both beams overlap ($L_b + \Delta L$) as the test. The angular size of the test is the same as the probe. At the observer's pupil, the background field subtends 1° and the probe subtends 0.5° [Fig. 1(a)].

The light source employed in this work was an incandescent halogen lamp with a color temperature of 2857 K. Spectral distribution of the lamp is shown in Fig. 1(b). Several shutters controlled the stimulus and the fixation test exposure times as well as the delay between them. The uncertainty in the timing control was measured with a photodiode and was less than 1 ms. Neutral density filters controlled the luminance of the background and the probe beams stepped in 0.1 log units. Luminances were measured with a Spectra Pritchard 1980 luminance meter. During measurements, the observer's head was fixated to the setup with the use of a bite bar made of a dental compound. The observer's face was illuminated with infrared LEDs (830 nm) and the pupil was imaged with a CCD camera

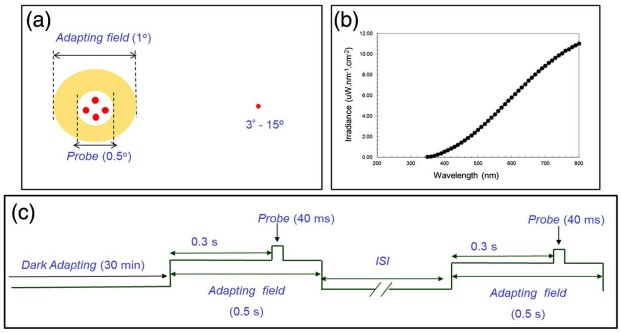

Fig. 1. Experimental configuration. (a) contains a diagram of the spatial arrangement. The spectral distribution of the incandescent lamp with tungsten filament used to produce the visual stimulation is shown in (b). The temporal sequence for transient light adapting condition with 300 ms delay between the beginning of the adapting field and the probe is represented in (c).

in order to verify that its size was greater than the imaged filament (2 mm × 1 mm). Before any trial or measurement, the observer's pupil was centered on the plane containing the two overlapped images of the filament (one for each beam).

B. Subjects

The tenets of the Declaration of Helsinki were followed. Three subjects (AG, IA, and CB; two females and one male) participated in the study with ages 27, 38, and 40 years. All participants passed an ophthalmological examination including refraction, ocular media, and fundus assessment. No pathologies or ocular opacities were observed. The best optical refraction for far distance was employed in all cases in order to obtain visual acuities logMar 0.0 or better. All measurements were performed on the temporal retina of the right eye while the left eye was occluded.

C. Procedure and Measurements

Before contrast threshold measurements were obtained, the observers were adapted to darkness (5×10^{-6} cd/m^2) for 30 min. Then the probe was presented for 40 ms, 300 ms after the onset of the adapting field, which lasted for 500 ms [Fig. 1(c)]. Therefore this experiment followed the stimulus onset asynchrony (SOA) paradigm. The observer's task was to report whether they detected the probe or not. The interstimulus interval (ISI) was 10 s for all of the background luminance levels, except for $L_b \geq 15$ cd/m^2 in which the ISI was increased to 30 s in order to avoid afterimages [11].

In all cases, the subject's fixation was maintained on the proper fixation mark during light adaptation and during measurements. The foveal measurement fixation test consisted of four dim red fixation points in a diamond configuration whereas, for extrafoveal measurements, a single dim fixation point was employed. In all cases, small light emitting diodes (LEDs, central wavelengths at 630 nm) were used. A limits method was employed for all measurements. In this method, a staircase procedure was employed. A series began with a stimulus intensity below the threshold, and then the stimulus intensity was increased in 0.1 log units until it reached the

upper limit. The threshold for this series was estimated as the midpoint between the stimulus intensities for the last NO response and the first YES response. Then a series began with the stimulus intensity at the upper limit, so the stimulus intensity was decreased in 0.1 log units until it reached the lower limit. The threshold for this series was estimated as the midpoint between the stimulus intensities of the last YES response and the first NO response. Runs were performed as ascending or descending in a random way. The threshold was finally estimated as the average of the previously calculated midpoints, which was always an equal number of ascending and descending staircases. In addition, in the mesopic range, the results were compared with the constant stimuli method. In these cases, a preliminary estimation of the luminance threshold was obtained with the limits method. Five probe luminances near the estimated threshold were repeated randomly 20 times each. Afterwards, the final threshold, ΔL, was obtained from the psychometric curve. Differences between this value and the previously obtained value by the limits method were, in the most unfavorable case, lower than 0.15 log units. A similar procedure was performed in our previous studies [16,25].

All measurements were carried out for 0°, 3°, 6°, 9°, 12°, and 15° of eccentricity [with respect to fixation, Fig. 1(a)]. For background luminances 0.06, 0.6, and 5 cd/m^2, pupil diameters were around or greater than 4 mm for all subjects. This is the luminance that is considered to be the mesopic-to-photopic transition luminance. For 15, 25, 40, 65, 80, and 100 cd/m^2, a mydriatic was employed (tropicamide 1%, Colircusi Alcon) in order to avoid pupil effects on retinal illumination. In these cases pupil diameters were always near or greater than 7 mm. Light levels expressed as retinal illuminance values are shown in Table 1. The photopic retinal illuminances (in photopic trolands) can be simply obtained by multiplying the photopic luminances (in photopic cd/m^2) by the filament area (2 mm^2) used in a Maxwellian optical system. Photopic trolands and scotopic trolands at 10° were computed using the Smith and Pokorny [26] fundamentals and the scotopic luminosity function, respectively, as explained elsewhere [27].

Statistical analyses were performed on data using the software STATA 12.0 (StataCorp LP, College Station, TX). In order to avoid bias we took these precautions: session times shorter than one and half hours and optimal physical and psychological conditions of the subjects. Data screening considered assessment of outliers, normality, and homogeneity of variances. Although there is not a minimum sample size for the statistical analysis implemented, problems due to small sample size could arise to reject a false null hypothesis; however, in our analyses the null hypothesis has been rejected in all cases.

Table 1. Light Levels Expressed in cd/m^2 and Trolands

Background Light Level (Lb)			
cd/m^2	Photopic td	Photopic td 10°	Scotopic td 10°
0.06	0.12	0.13	0.08
0.65	1.2	1.26	0.81
5	10	10.54	6.75
15	30	31.61	20.24
25	50	52.68	33.73
40	80	84.29	53.98
65	130	137	87.71
80	160	168.6	108
100	200	210.7	134.9

3. RESULTS

A. Tvl Curves

Threshold results, expressed as the luminance of the probe in a function of the background luminance, for the three subjects are shown in Fig. 2. A repeated measures analysis of variance showed significant differences among eccentricities [$F(5, 65) = 7.48$, $p < 0.01$]. For all eccentricities, thresholds increased with L_b; however, there were different trends. In general, thresholds increased with eccentricity as expected. Weber's law can be used to describe the contrast threshold for foveal steady adapting conditions [LA (0°)]; however, for transient conditions, a different behavior was found. Curves seem to be formed by different branches with different slopes for the mesopic and photopic ranges, and are principally marked for 6° and 9°. Particularly interesting is the data trend for 6°, which is similar to the 0° and 3° data behavior for mesopic conditions. However, when increasing light levels to the photopic range, data for 6° became similar to 9°, 12°, and 15° data (Fig. 2).

Since the three subjects' data showed similar trends, we averaged them for subsequent analyses. In Fig. 3, we plotted the averaged results for each eccentricity together with the data for steady conditions ($n = 3$) from Gloriani and colleagues [16]. All curves for the transient conditions are mostly above the data for the steady conditions at the same eccentricity, which indicates that contrast sensitivity was lower in the transient versus steady conditions. Interestingly, in comparison with the steady data, the 6° transient data showed higher sensitivity at a high mesopic level (5 cd/m^2), and the same tendency might happen at 9°. At photopic light levels, the difference between transient and steady data was more notable ($df = 1$, $F = 162.95$, $p < 0.001$) than the difference at mesopic levels ($df = 1$, $F = 5.29$, $p < 0.05$), but both were significant. A Tukey's postestimation analysis showed that the

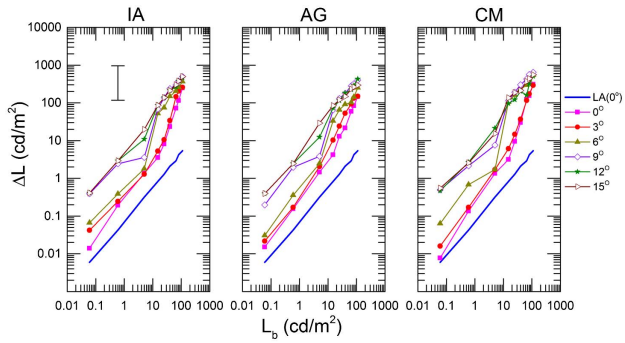

Fig. 2. Contrast threshold results with transient adapting backgrounds ranging from mesopic to photopic levels at different eccentricities. Each panel contains results expressed as luminance of the probe (ΔL) for each subject. The solid line represents the average contrast threshold for foveal steady adapting conditions (LA, from Gloriani *et al.* [16]); it is included for reference purposes. The estimated uncertainty (±0.15 log units) is displayed in the first panel.

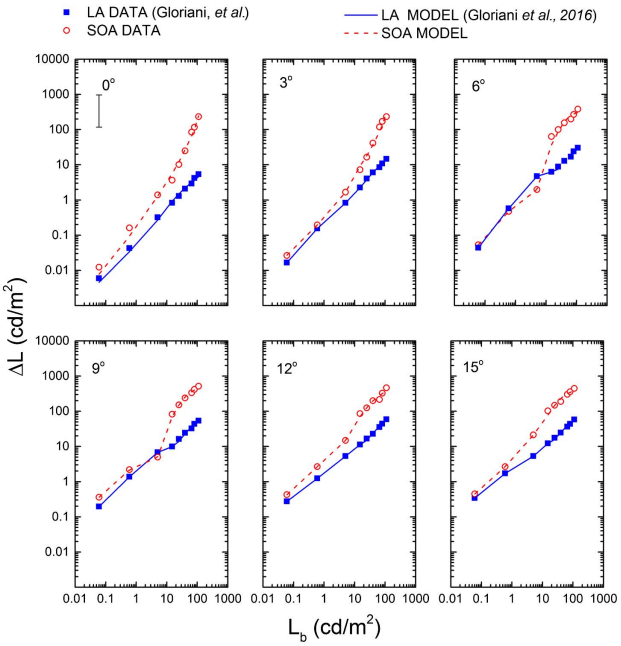

Fig. 3. Average of SOA results compared with LA results. Lines represent the model for both conditions. Each panel is for a different eccentricity. The estimated uncertainty (±0.15 log units) is displayed in the first panel.

only difference occurred at 5 cd/m^2 ($t = -3.45$; $p < 0.05$) and not for 0.6 cd/m^2 ($t = -0.49$; $p = 0.996$) or for 0.06 cd/m^2 ($t = -0.07$; $p = 1$).

B. Adaptation Recovery

Changes in sensitivity between transient and steady conditions can be compared in terms of adaptation recovery (Ar), which is computed as the ratio of the results at steady conditions to the results at transient conditions expressed in log units [25,28], Eq. (1). When our index was close to zero, it indicated that adaptation was achieved in a period of time as short as 300 ms. Negative values indicated that sensitivity has not yet recovered:

$$Ar = \log_{10}\left(\frac{\Delta L_{\mathrm{LA}}}{\Delta L_{\mathrm{SOA}}}\right). \tag{1}$$

Different predictions can outline the light adaptation timing, considering the effect of eccentricity and light level in terms of adaptation recovery. For example, if adaptation processing is completed, the adaptation recovery index is close to zero [Fig. 4(a)]. If for all eccentricity–light level combinations there is similar partial adaptation, the adaptation recovery index will be less than zero, Fig. 4(b)]. We can also predict how adaptation recovery depends on light level only [Fig. 4(c)] or on eccentricity only [Fig. 4(d)].

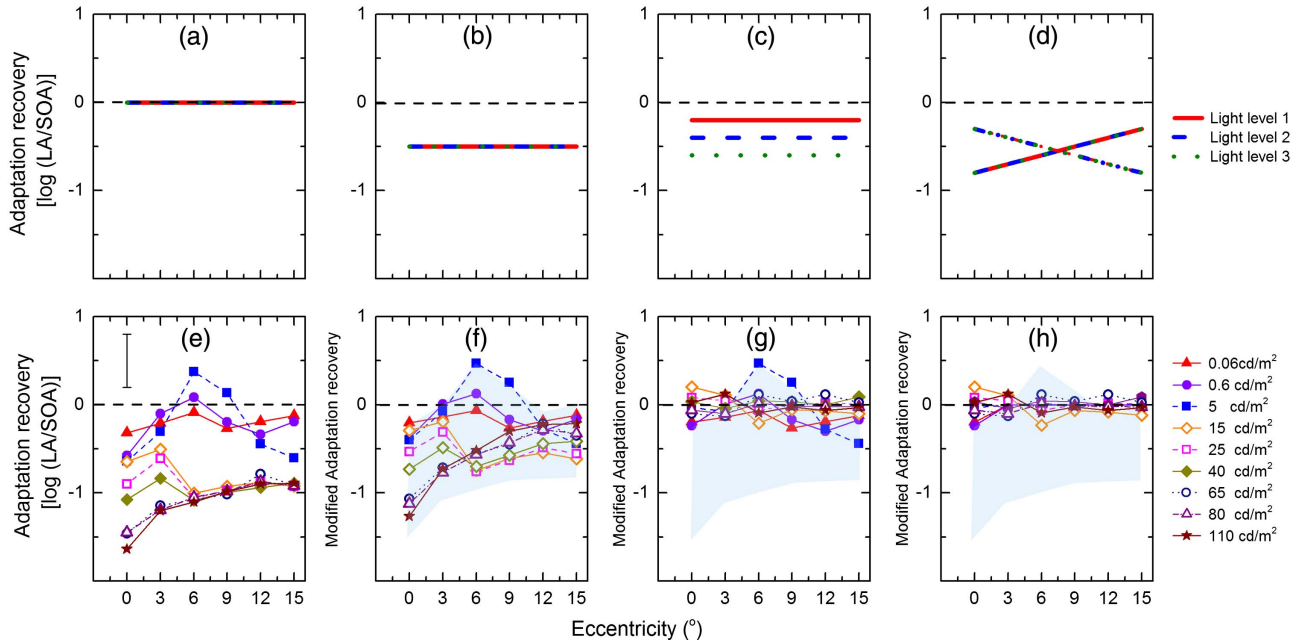

Fig. 4. Adaptation recovery analysis. (a)–(d) contain four predictions for the adaptation recovery according to different hypotheses for the timing of adaptation processing: (a) same adaptation in transient and steady data; (b) worse adaptation in transient than steady conditions independent of light level and retinal location; timing dependent only on (c) light level or (d) eccentricity. (e) Adaptation recovery results computed from current transient data and from Gloriani and colleagues for steady conditions [16]. (f)–(h) show the effect of changing parameter values in the model used by Gloriani and colleagues to explain transient data. These points were obtained using the model prediction including different corrections instead of steady data in Eq. (1). (f) Correcting only subtractive (S) and molecular mechanisms (M); (g) including the cone gain control mechanism (g, M, and S); and (h) including noise intrusion (N, g, M, S). In this way the contribution of each mechanism is evident to explain transient data with respect to steady data. Shadow areas in (f)–(h) represent the spread for the adaptation recovery data of (e).

In Fig. 4(e), logarithmic changes of adaptation recovery computed for our data as a function of eccentricity for all light levels are shown.

Four different adaptive behaviors can be recognized from Fig. 4(e). Behavior 1: At low light levels (0.06 and 0.6 cd/m^2), independent from eccentricity, there is not much difference between LA and SOA results, with transient thresholds a little bit higher than the steady results for most eccentricities [similar to the prediction in Fig. 4(a)]. Behavior 2: Photopic results beyond the fovea share the same degree of partial adaptation independent of both eccentricity and light level [similar to the prediction in Fig. 4(b)]. Behavior 3: Foveal adaptation, instead, depends on the intensity of the background; adaptation recovery is reduced with increasing light levels [similar to the prediction in Fig. 4(c)]. Behavior 4: Adaptation at a high mesopic luminance level (5 cd/m^2) depends on the eccentricity in a complex manner; adaptation is reduced in transient conditions for the fovea and peripheral regions beyond 9°, but surprisingly for 6° and 9°, the logarithmic of this ratio was higher than 0. This behavior resembles the prediction of Fig. 4(d).

This analysis showed that the variation between transient and steady conditions is different across light levels and eccentricities, which is evidence of different timing in the involved mechanisms of adaptation.

4. MODEL

The analysis on adaptation recovery showed the complexity of the adaptation process considering light level and retinal location. In order to understand the timing of the adaptation mechanisms involved in this complex adaptive behavior, we used a mechanistic model developed previously for steady conditions [16]. The model predicted luminance threshold values (ΔL) for transient backgrounds, where ΔL values come from the following expression [Eq. (2)]:

$$\Delta L = \left\{ \frac{\sigma_T'^n}{\frac{1}{\left[\frac{C_n R(L_b)}{G_c}\right] + R(L_b)} - 1} \right\}^{1/n} + S + N - L_b. \quad (2)$$

With $C_n = 0.01$ as the minimum Weber contrast necessary for detection, this expression proposed by Gloriani and colleagues [16] describes different mechanisms. Contrast gain (G_c), defined as the ratio of a change in visual response to a contrast change in the stimulation, did not change for transient conditions. We assumed that the mechanism controlling contrast gain (G_c) is completed at 300 ms since there is evidence of a fast contrast gain control mechanism [29]; therefore, we did not modify the values used in Gloriani and colleagues' article [16]. Instead, we modified the behavior of other mechanisms involved in the temporal light adaptation process as subtractive (S), molecular (M), and gain control (g) as well as noise intrusion (N). Subtractive mechanism actions, which reduce the background luminance, are dependent on time [13,15], and, at 300 ms, their action is not completed {Eq. (A.5) in Gloriani *et al.* [16]}. Other parameters involved in the subtractive mechanism depending on both eccentricity and the background adaptation size remain unchanged in the model from steady conditions. On the other hand, the molecular mechanism involved in gain control {Eq. (A.7) in Gloriani *et al.* [16]} is not active in transient conditions because it is sluggish [30]. However, these changes from the model implemented with LA data to the modeling implemented with SOA results are minor, as shown in Fig. 4(f).

Gain control and noise intrusion are significant in the timing of adaptation; their effects are shown in Figs. 4(g) and 4(h), respectively. In the model [Eq. (2)], there are parameters such as the Hill constant (n) and test half saturation (σ_T'), which are involved in the nonlinear retinal cell responses (R) [31]. Further details of the expressions involved in the modeling can be found in our previous works [15,16]. We explain the modifications of the model in more detail in the following sections.

A. Dependence of Gain Control with Eccentricity

Gain control mechanism parameters that were used previously [16] are based on physiological data obtained at steady conditions for one retinal location [32]. We changed the parameters of the gain control mechanism for cones in order to account for timing and eccentricity.

Gain control, implicit in cell responses, is included following the proposal of Dunn and colleagues [33] for the steady condition [Eq. (3)]:

$$g = \left(\frac{|a| + bI_b}{|a| + I_b} \right) (cI_b + 1)^m. \quad (3)$$

The term on the left side of Eq. (3) is for gain control (g). On the right side, the term a determines the intensity at which the increase begins, and b is the amount of increase. The second term describes the decreased amplitude with background, with c setting when the decrease begins. I_b is the background intensity; m describes the dependence between gain control and background.

In order to find the response for the transient condition, at first we analyzed the gain control in the fovea, where only cones are present [34]. Therefore, the parameters c and m have been used as free parameters to fit the model to the experimental data in both mesopic and photopic luminance ranges. The rest of the parameters were proposed by Dunn and colleagues [33].

We observed that gain control was similar to that suggested by Dunn in photoreceptor gain control [Fig. 5(a)]. In parafoveal conditions, for each eccentricity, the parameters c and m have been used to fit the model to the experimental data in the photopic luminance range, where only cones are active.

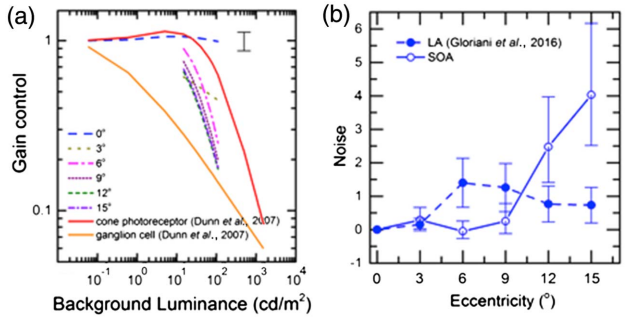

Fig. 5. (a) Gain control mechanism function implemented in our model for different retinal eccentricities (see Data File 1 for parameter values). (b) Noise intrusion at 5 cd/m^2 for transient (SOA) and steady (LA) conditions.

The behavior of gain control responses trending from photoreceptors to ganglion cells with eccentricity is evident [Fig. 5(a)].

This analysis showed that the place of adaptation changes from photoreceptors to ganglion cells in a gradual manner with eccentricity. Since cone gain is controlled by light level, this mechanism accounts mostly for behavior 3 [Fig. 4(g)].

B. Noise Intrusion

Based on our previous findings, noise intrusion is evident for mesopic levels [16]. We modeled noise intrusion (N) as a parameter that affects the detection of the test. The model showed that noise in transient conditions is higher than noise in steady conditions for high eccentricities, but lower for 5 cd/m^2 between 6° and 9° [Fig. 5(b)]. It is associated with the lower threshold for the transient condition than for the steady condition at 5 cd/m^2 and 6° and 9°, as observed in Fig. 3. Thus noise intrusion depends on eccentricity; therefore, it explains behavior 4 and behavior 1 to a minor extent [Fig. 4(h)].

The model with the parameter values updated for transient conditions is shown in Fig. 3. The goodness of fit of our model for this condition was very good for all the eccentricities ($\chi^2 = 0.99$; with maximum standard deviation for 0°: $\pm$ 0.133). Also, Fig. 4(h) represents the effect of the complete model with respect to transient data. Values of parameters for steady and transient conditions are provided in Data File 1.

5. DISCUSSION

Adaptation recovery varies with both retinal locations and light levels. Light adaptation is equally faster at low light levels (0.06 and 0.6 cd/m^2) for different retinal locations. At the fovea, adaptation recovery is a function of the light level. Adaptation slows with extrafoveal eccentricity for high mesopic luminance. Photopic extrafoveal (from 6°) thresholds are one log unit higher for transient than steady conditions, independent of light level and eccentricity. These behaviors are explained by different timing of the mechanisms involved in adaptation, and this concept is developed in our modeling.

At photopic conditions, one would expect a behavior similar to the prediction of Fig. 4(b), where only subtractive and molecular mechanisms would change from steady to transient conditions. However, the different behaviors between the fovea and extrafovea was surprising [Fig. 4(e)]. In fact, in the extrafoveal region, the behavior was similar to Fig. 4(b), while in the fovea and at 3° it depended on the light level, which is similar to the prediction in Fig. 4(c). The transition between both behaviors is not smooth but switches. This difference can be explained by a change in the site of multiplicative adaptation [Fig. 5(a)]. It is known that there exist two sites of cone light adaptation in the retina; one is receptoral [35] and, therefore, intrinsic to the photoreceptor, and the other one is postreceptoral [36]. Dunn and colleagues have located the site of postreceptoral adaptation in the synapsis between bipolar and ganglion cells [33]. Although it was proposed that the site of this multiplicative adaptation is postreceptoral for steady conditions [16] and for foveal mesopic transient levels [15], our results suggest that, at foveal photopic transient levels, the site of multiplicative adaptation is mostly in the cones. In our model, two parameter values of the cone gain control mechanism differ by one log unit for the fovea than for the extrafovea; this difference explains the different behaviors of the model with eccentricity. Gain control in the fovea is near unity, showing cone saturation. It is known that saturation is associated with transient adaptation [37], which reinforces our results. In this case, light adaptation is not completed in 300 ms.

Cone gain control sites switch with light levels. Dunn and colleagues showed that for high photopic levels, light adaptation is receptoral, however, for lower light levels, adaptation in cones switches to postreceptoral circuitry [33]. Although it was not identified by physiological studies, we propose a change in the site of cone gain control mechanisms with eccentricity for transient conditions at photopic levels. Specifically, in the central region, the predominant site of adaptation would be in the cones, but in the periphery, the predominance of gain control would be located in the cone bipolar synapses with ganglion cells, which is convenient because a postreceptoral site of adaptation in the periphery benefits from higher convergence of cone cells to parasol ganglion cells [38].

At mesopic light levels, we also found two nonexpected behaviors. At 5 cd/m^2, transient sensitivity is higher than steady sensitivity for 6° and 9° of eccentricity, which is reflected as a positive adaptation recovery [Fig. 4(e)]. In our model, this light level represents the transition zone between photopic and mesopic light levels. Our explanation for this complex behavior considers noise intrusion to be minimal from 6° to 9° in transient conditions [See Fig. 5(b)], whereas there is a higher noise effect in steady conditions. This behavior suggests noise temporal evolution [2], which can be explained considering the involvement of an adaptive mechanism sensitive to noise working at high mesopic levels, which is not completed at 300 ms. Evidence of this type of mechanism was found psychophysically in humans [24] and physiologically in toads [39]. Specifically, Brown and Rudd [24] showed that the action of this mechanism is evident for brief and small stimuli such as those used in our study. This mechanism could be related to cone–rod interactions, principally for small size test and background stimuli, similar to other experiments [40]. It is known that the surrounding rods modify the amplitude and latency times of peripheral cones [41–43]. In a recent work, Zele and colleagues showed rod–cone interactions are longer than cone–cone interactions due to the different response times of rods and cones [44]. Therefore, at 300 ms, noise could not influence the signal responses due to incomplete interactions. On the other hand, it should be noted that, in our model, noise is additive; therefore, it always increased thresholds [Fig. 5(b)]. However, it was recently shown that, at mesopic light levels, rod sensitivity is affected differently, depending on the nature of the noise correlation and duration of the detection test [45]. Our noise modeling approach, considering our test duration (40 ms), is in agreement with the conclusions of Hathibelagal and colleagues, since they showed that correlated pathway-specific noise and uncorrelated white noise for pulses shorter than 100 ms both increased rod thresholds [45].

At lower light levels, there is no significant difference between results from steady and transient conditions, meaning

that the transient component of adaptation responses (at least at 300 ms) is not as substantial in mesopic vision as it is in photopic vision. This behavior is counterintuitive, since rod involvement in mesopic vision should slow the response because of their intrinsic delay with respect to cones [46,47]. However, this delay (~12–20 ms for mesopic conditions [48]) was more than one log unit lower than our SOA time. Therefore, rod delay does not affect the results, and the main reason for small differences at low light levels is increased noise intrusion in transient conditions.

Our model, which was developed previously for steady conditions [16] and for brightness matching [15], can explain the experimental data for transient luminance detection thresholds. This model allowed analysis of the different mechanisms involved in rapid light adaptation.

The difference among the curves in Fig. 2 could be minimized by changing the SOA time. For several conditions, a longer SOA time, as expected, would increase the adaptation recovery times. Bichao and colleagues estimated that 500 ms is enough time to achieve complete adaptation at foveal conditions, but this time is not enough in the periphery [49]. However, Matesanz and colleagues showed that, in the high mesopic range between 6° and 9°, SOA times between 150 and 300 ms are enough to get complete adaptation [25]. Our work focused only on one SOA time spanning a high range of light levels and locations, and we showed how different adaptation recovery could be in those combined conditions. It would be interesting, especially for lighting regulations, to know which SOA time is enough in each condition to achieve complete adaptation; however, this question is beyond the purposes of this study.

Funding. Ministerio de Economía y Competitividad (MINECO) (FIS2016-78037-P); Consejo Nacional de Investigaciones Científicas y Técnicas (CONICET) (PIUE 0114).

Acknowledgment. Dr. J. A. Aparicio expresses his personal acknowledgment to the Organización Nacional de Ciegos de España (ONCE) for help.

Dr. Juan Aparicio (Apa) passed away during the revision process of this paper after a long illness. The other authors want to acknowledge his guidance throughout this research, which, in addition to the current paper, involved two other papers [16,25]. He had a leading role from the beginning of this project, providing original ideas, setting up the experimental apparatus, and becoming highly involved in the modeling of the data. His thoughtful comments on this paper until the end of his days were crucial for the success of the present work.

REFERENCES

1. A. Reeves, "Visual adaptation," in *The Visual Neurosciences*, L. M. Chalupa and J. S. Werner, eds. (MIT, 2004), pp. 851–862.
2. F. Rieke and M. E. Rudd, "The challenges natural images pose for visual adaptation," Neuron **64**, 605–616 (2009).
3. Y. V. Wang and J. B. Demb, "Postreceptoral mechanisms for adaptation in the retina," in *The New Visual Neurosciences*, J. S. Werner and L. M. Chalupa, eds. (MIT, 2014).
4. A. J. Zele and D. Cao, "Vision under mesopic and scotopic illumination," Front. Psychol. **5**, 1594 (2015).
5. J. B. Demb and J. H. Singer, "Functional circuitry of the retina," Annu. Rev. Vis. Sci. **1**, 263–289 (2015).
6. W. S. Stiles, "Color vision: the approach through increment-threshold sensitivity," Proc. Natl. Acad. Sci. USA **45**, 100–114 (1959).
7. W. S. Stiles, *Mechanisms of Colour Vision* (Academic, 1978).
8. D. C. Hood, "Lower-level visual processing and models of light adaptation," Annu. Rev. Psychol. **49**, 503–535 (1998).
9. R. Shapley and C. Enroth-Cugell, "Visual adaptation and retinal gain controls," Prog. Retin. Res. **3**, 263–346 (1984).
10. D. I. A. MacLeod, "Visual sensitivity," Annu. Rev. Psychol. **29**, 613–645 (1978).
11. E. H. Adelson, "Saturation and adaptation in the rod system," Vis. Res. **22**, 1299–1312 (1982).
12. W. S. Geisler, "Effects of bleaching and backgrounds on the flash response of the cone system," J. Physiol. **312**, 413–434 (1981).
13. H. R. Wilson, "A neural model of foveal light adaptation and afterimage formation," Visual Neurosci. **14**, 403–423 (1997).
14. H. P. Snippe, L. Poot, and J. H. van Hateren, "A temporal model for early vision that explains detection thresholds for light pulses on flickering backgrounds," Visual Neurosci. **17**, 449–462 (2000).
15. P. A. Barrionuevo, E. M. Colombo, and L. A. Issolio, "Retinal mesopic adaptation model for brightness perception under transient glare," J. Opt. Soc. Am. A **30**, 1236–1247 (2013).
16. A. H. Gloriani, B. M. Matesanz, P. A. Barrionuevo, I. Arranz, L. Issolio, S. Mar, and J. A. Aparicio, "Influence of background size, luminance and eccentricity on different adaptation mechanisms," Vis. Res. **125**, 12–22 (2016).
17. D. C. Hood and M. A. Finkelstein, "Sensitivity to light," Handb. Percept. Hum. Perform. **1**, 1–66 (1986).
18. G. Osterberg, *Topography of the Layer of Rods and Cones in the Human Retina* (Nyt Nordisk Forlag, 1935).
19. C. A. Curcio, K. R. Sloan, R. E. Kalina, and A. E. Hendrickson, "Human photoreceptor topography," J. Comp. Neurol. **292**, 497–523 (1990).
20. J. D. Crook, O. S. Packer, J. B. Troy, and D. M. Dacey, "Synaptic mechanisms of color and luminance coding: rediscovering the XY-cell dichotomy in primate retinal ganglion cells," in *The New Visual Neurosciences* (MIT, 2014), pp. 123–143.
21. D. F. Garway-Heath, J. Caprioli, F. W. Fitzke, and R. A. Hitchings, "Scaling the hill of vision: the physiological relationship between light sensitivity and ganglion cell numbers," Invest. Ophthalmol. Visual Sci. **41**, 1774–1782 (2000).
22. C. Huchzermeyer and J. Kremers, "Perifoveal L- and M-cone-driven temporal contrast sensitivities at different retinal illuminances," J. Opt. Soc. Am. A **33**, 1989–1998 (2016).
23. C. Huchzermeyer and J. Kremers, "Perifoveal S-cone and rod-driven temporal contrast sensitivities at different retinal illuminances," J. Opt. Soc. Am. A **34**, 171–183 (2017).
24. L. G. Brown and M. E. Rudd, "Evidence for a noise gain control mechanism in human vision," Vis. Res. **38**, 1925–1933 (1998).
25. B. M. Matesanz, L. A. Issolio, I. Arranz, C. de la Rosa, J. A. Menéndez, S. Mar, and J. A. Aparicio, "Temporal retinal sensitivity in mesopic adaptation," Ophthalmic Physiol. Opt. **31**, 615–624 (2011).
26. V. C. Smith and J. Pokorny, "Spectral sensitivity of the foveal cone photopigments between 400 and 500 nm," Vis. Res. **15**, 161–171 (1975).
27. P. A. Barrionuevo and D. Cao, "Contributions of rhodopsin, cone opsins, and melanopsin to postreceptoral pathways inferred from natural image statistics," J. Opt. Soc. Am. A **31**, A131–A139 (2014).
28. H.-W. Bodmann, R. Greule, and S. Kokoschka, "Contrast thresholds at transient adaptation," in *Proceeding of 22nd Session of the CIE* (1991), Vol. **1**, pp. 25–28.
29. J. B. Demb, "Functional circuitry of visual adaptation in the retina," J. Physiol. **586**, 4377–4384 (2008).
30. A. Stockman, M. Langendörfer, H. E. Smithson, and L. T. Sharpe, "Human cone light adaptation: from behavioral measurements to molecular mechanisms," J. Vis. **6**(11), 1194–1213 (2006).
31. K. I. Naka and W. A. H. Rushton, "S-potentials from colour units in the retina of fish (Cyprinidae)," J. Physiol. **185**, 536–555 (1966).

32. F. A. Dunn and F. Rieke, "The impact of photoreceptor noise on retinal gain controls," Curr. Opin. Neurobiol. **16**, 363–370 (2006).
33. F. A. Dunn, M. J. Lankheet, and F. Rieke, "Light adaptation in cone vision involves switching between receptor and post-receptor sites," Nature **449**, 603–606 (2007).
34. S. Raphael and D. I. A. MacLeod, "Mesopic luminance assessed with minimum motion photometry," J. Vis. **11**(9):14, 1–21 (2011).
35. J. L. Schnapf, B. J. Nunn, M. Meister, and D. A. Baylor, "Visual transduction in cones of the monkey Macaca fascicularis," J. Physiol. **427**, 681–713 (1990).
36. B. B. Lee, J. Pokorny, P. R. Martin, A. Valbergt, and V. C. Smith, "Luminance and chromatic modulation sensitivity of macaque ganglion cells and human observers," J. Opt. Soc. Am. A **7**, 2223–2236 (1990).
37. M. A. Finkelstein and D. C. Hood, "Cone system saturation: more than one stage of sensitivity loss," Vis. Res. **21**, 319–328 (1981).
38. A. K. Goodchild, K. K. Ghosh, and P. R. Martin, "Comparison of photoreceptor spatial density and ganglion cell morphology in the retina of human, macaque monkey, cat, and the marmoset Callithrix jacchus," J. Comp. Neurol. **366**, 55–75 (1996).
39. K. Donner, D. R. Copenhagen, and T. Reuter, "Weber and noise adaptation in the retina of the toad Bufo marinus.," J. Gen. Physiol. **95**, 733–753 (1990).
40. G. Lange, N. Denny, and T. E. Frumkes, "Suppressive rod-cone interactions: evidence for separate retinal (temporal) and extraretinal (spatial) mechanisms in achromatic vision," J. Opt. Soc. Am. A **14**, 2487–2498 (1997).
41. A. J. Zele, D. Cao, and J. Pokorny, "Rod-cone interactions and the temporal impulse response of the cone pathway," Vis. Res. **48**, 2593–2598 (2008).
42. D. Cao, B. B. Lee, and H. Sun, "Combination of rod and cone inputs in parasol ganglion cells of the magnocellular pathway," J. Vis. **10**(11):4, 1–15 (2010).
43. J. Pokorny and D. Cao, "Rod and cone contributions to mesopic vision," in *CIE Symposium "Lighting Quality & Energy Efficiency", X035* (2010), pp. 9–20.
44. A. J. Zele, M. L. Maynard, and B. Feigl, "Rod and cone pathway signaling and interaction under mesopic illumination," J. Vis. **13**(1):21, 1–19 (2013).
45. A. R. Hathibelagal, B. Feigl, J. Kremers, and A. J. Zele, "Correlated and uncorrelated invisible temporal white noise alters mesopic rod signaling," J. Opt. Soc. Am. A **33**, A93–A103 (2016).
46. A. Stockman and L. T. Sharpe, "Into the twilight zone: the complexities of mesopic vision and luminous efficiency," Ophthalmic Physiol. Opt. **26**, 225–239 (2006).
47. L. T. Sharpe, A. Stockman, and D. I. A. MacLeod, "Rod flicker perception: scotopic duality, phase lags and destructive interference," Vis. Res. **29**, 1539–1559 (1989).
48. D. M. Schneeweis and J. L. Schnapf, "Photovoltage of rods and cones in the macaque retina," Science **268**, 1053–1056 (1995).
49. I. C. Bichao, D. Yager, and J. Meng, "Disability glare: effects of temporal characteristics of the glare source and of the visual-field location of the test stimulus," J. Opt. Soc. Am. A **12**, 2252–2258 (1995).